

Bose-Einstein condensates in standing waves: The cubic nonlinear Schrödinger equation with a periodic potential

Jared C. Bronski¹, Lincoln D. Carr^{2*}, Bernard Deconinck³, and J. Nathan Kutz³

¹*Department of Mathematics, University of Illinois Urbana-Champaign, Urbana, IL 61801, USA*

²*Department of Physics, University of Washington, Seattle, WA 98195-1560, USA*

³*Department of Applied Mathematics, University of Washington, Seattle, WA 98195-2420, USA*

We present a new family of stationary solutions to the cubic nonlinear Schrödinger equation with a Jacobian elliptic function potential. In the limit of a sinusoidal potential our solutions model a dilute gas Bose-Einstein condensate trapped in a standing light wave. Provided the ratio of the height of the variations of the condensate to its DC offset is small enough, both trivial phase and nontrivial phase solutions are shown to be stable. Numerical simulations suggest such stationary states are experimentally observable.

The dilute-gas Bose-Einstein condensate (BEC) in the quasi-one-dimensional regime is modeled by the cubic nonlinear Schrödinger equation (NLS) with a potential [1–3]. The various traps which are used to contain the BEC have spurred the solution of the NLS with new potentials [4,5]. BECs trapped in a standing light wave have been used to study phase coherence [6] and matter-wave diffraction [7] and have been predicted to have applications in quantum logic [8] and matter-wave transport [9]. Exact solutions have been obtained for the Kronig-Penney potential [10] and some researchers have used a Bloch function description [11]. In this letter, we study new explicit solutions of the NLS with a Jacobian elliptic function potential.

We consider the mean-field model of a quasi-one-dimensional repulsive BEC trapped in an external potential which is given by the nonlinear Schrödinger equation [1]

$$i\psi_t = -\frac{1}{2}\psi_{xx} + |\psi|^2\psi + V(x)\psi. \quad (1)$$

In experiments, the trapping potential is generated by a standing light wave [6]. As a model for such a potential we use the periodic potential

$$V(x) = -V_0 \operatorname{sn}^2(x, k) \quad (2)$$

where $\operatorname{sn}(x, k)$ denotes the Jacobian elliptic sine function [12] with elliptic modulus $0 \leq k \leq 1$. In the limit $k \rightarrow 1^-$, $V(x)$ becomes an array of well-separated hyperbolic secant potential barriers or wells, while in the limit $k \rightarrow 0^+$ it becomes purely sinusoidal. We note that for intermediate values (e.g. $k = 1/2$) the potential closely resembles the sinusoidal behavior and thus provides a good approximation to the standing wave potential generated experimentally [6].

We present stationary solutions in closed form and study their stability analytically and numerically. We begin by constructing solutions to Eq. (1) which have the form

$$\psi(x, t) = r(x) \exp(i(\Theta(x) - \omega t)) \quad (3)$$

where

$$r^2(x) = (V_0 + k^2) \operatorname{sn}^2(x, k) + B \quad (4a)$$

$$\Theta(x) = c \int_0^x \frac{dx'}{r^2(x')} \quad (4b)$$

$$\omega = \frac{1}{2} \left(1 + k^2 + 3B - \frac{BV_0}{k^2 + V_0} \right) \quad (4c)$$

$$c^2 = B \left(1 + \frac{B}{k^2 + V_0} \right) (k^2 + V_0 + Bk^2) \quad (4d)$$

where B determines a mean amplitude and acts as a DC offset for the number of condensed atoms. The strength of the nonlinearity, which for the BEC is a function of both the atomic coupling and the number of condensed atoms, is determined by the parameters $V_0 + k^2$ and B , as is apparent in the amplitude of the solutions given by Eq. (3). Note that if x is scaled so that $V(x)$ undergoes only a single oscillation on the ring (in the limit $k \rightarrow 1$) the Jacobian elliptic potential provides a model of a single barrier or well [13]. For simplicity we focus on two special cases: (1) k arbitrary and trivial phase ($c = 0$), and (2) $k = 0$ with nontrivial phase ($c \neq 0$) so that the solutions are trigonometric functions.

Trivial Phase Case – In the limit of $c = 0$, the solutions given in Eqs. (3)-(4) reduce to

$$\psi(x, t) = \sqrt{V_0 + k^2} \operatorname{sn}(x, k) \exp[-i(1 + k^2)t/2] \quad (5)$$

valid for $V_0 \geq -k^2$, and

$$\psi(x, t) = \sqrt{-(V_0 + k^2)} \operatorname{cn}(x, k) \exp[-i(V_0 + k^2 - \frac{1}{2})t], \quad (6a)$$

$$\psi(x, t) = \sqrt{-(1 + \frac{V_0}{k^2})} \operatorname{dn}(x, k) \exp[i(1 + \frac{V_0}{k^2} - \frac{k^2}{2})t] \quad (6b)$$

valid for $V_0 \leq -k^2$ where $\operatorname{cn}(x, k)$ and $\operatorname{dn}(x, k)$ are Jacobian elliptic functions [12]. These solution branches

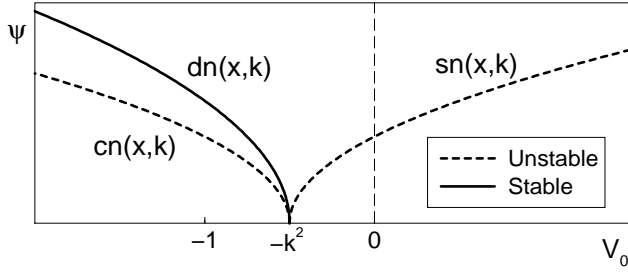


FIG. 1. Regions of validity for trivial phase Jacobian elliptic solutions. The $\text{sn}(x, k)$ and $\text{cn}(x, k)$ branches are found to be unstable while the $\text{dn}(x, k)$ branch is stable.

are illustrated in Fig. 1 along with their stability properties found from analytic calculations and observed in numerical simulation.

We can prove that the $\text{dn}(x, k)$ branch of solutions is linearly stable. To do so, we linearize about the $\text{dn}(x, k)$ solution branch given by Eq. (6b) so that

$$\psi(x, t) = (\phi_0(x) + \phi(x, t)) \exp(-i\omega t) \quad (7)$$

where $\phi_0(x) \exp(-i\omega t)$ is the exact solution given by Eq. (6b) and $\phi(x, t) \ll 1$ is a small perturbation to the exact solution. This leads to the following linearized eigenvalue problems

$$L_- L_+ R = \lambda^2 R \quad (8a)$$

$$L_+ L_- I = \lambda^2 I \quad (8b)$$

where $\phi(x, t) = (R + iI) \exp(i\lambda t)$ is decomposed into its real and imaginary parts. The operators L_- and L_+ are both self-adjoint and periodic differential operators:

$$L_- = \frac{1}{2} \partial_x^2 - \phi_0(x)^2 - V(x) - \omega \quad (9a)$$

$$L_+ = \frac{1}{2} \partial_x^2 - 3\phi_0(x)^2 - V(x) - \omega. \quad (9b)$$

Thus the eigenvalue problem closely resembles that of soliton solutions of the NLS [14] with the additional difficulty of $V(x)$ being a periodic potential.

We are able to prove stability for the whole $\text{dn}(x, k)$ branch of solutions and instability for the $\text{cn}(x, k)$ and $\text{sn}(x, k)$ branches near their emanation point $V_0 = -k^2$ (see Fig. 1). We note that stability or instability is proven by showing that the eigenvalue λ^2 in Eq. (8) is positive or negative respectively. For the $\text{dn}(x, k)$ branch of solutions, we find that L_+ is a positive definite operator. This allows us to construct its inverse. We then consider the related problem $L_- I = \lambda^2 L_+^{-1} I$ which is self-adjoint with respect to the weighting operator L_+^{-1} . This then allows us to show that $\lambda^2 > 0$ so that the eigenvalues remain real, establishing stability.

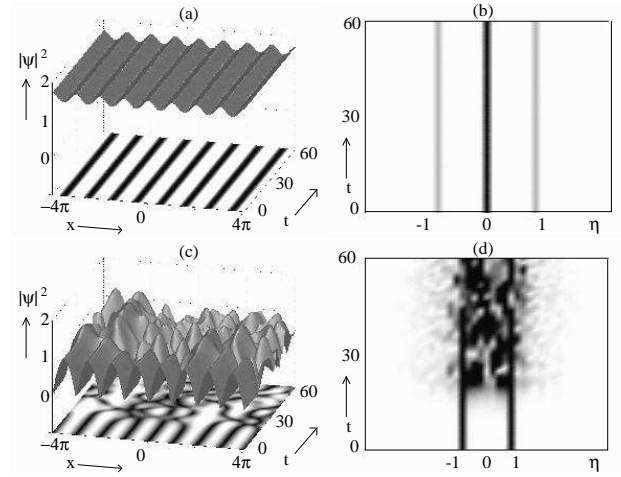


FIG. 2. Evolution of initially perturbed Jacobian elliptic $\text{dn}(x, k)$ and $\text{sn}(x, k)$ solutions. Panels (a)–(b) correspond to the stable $\text{dn}(x, k)$ branch of solutions of Fig. 1 with $k = 1/2$ and $V_0 = -1$. The wavenumber spectrum (η) remains constant and consists of the zero mode and wavenumber one. These reflect the DC offset and strength of oscillation, respectively. Panels (c)–(d) demonstrate the instability of the $\text{sn}(x, k)$ solution with $k = 0$ and $V_0 = 1$. Here the instability is seen to develop around wavenumber unity as predicted analytically. The $\text{cn}(x, k)$ branch of solutions exhibits the same instability.

In contrast to the $\text{dn}(x, k)$ solutions, numerical experiments suggest that all $\text{cn}(x, k)$ and $\text{sn}(x, k)$ solutions are linearly unstable. Although we have been unable to show this for the whole solution branch, we have shown this perturbatively for $V_0 + k^2 \ll 1$ using the same technique as outlined above for the $\text{dn}(x, k)$ branch of solutions. In this limit, the dispersion relation for small disturbances near $V_0 + k^2 \ll 1$ is

$$\omega^2 = \frac{(\eta^2 - 1)^2}{2} + C(V_0 + k^2) \frac{\eta^2 - 1}{2}, \quad (10)$$

where η is the wavenumber of the disturbance and C is a non-zero constant. From this it follows that there is a band of unstable modes which occurs near $\eta = 1$. Numerical experiments show that this unstable band persists for all V_0 and grows as $V_0 + k^2$ becomes large. We emphasize that the stable $\text{dn}(x, k)$ branch of solutions consists of oscillations about a non-zero mean value, while the unstable $\text{cn}(x, k)$ and $\text{sn}(x, k)$ branches have zero mean, suggesting that the offset has an important effect on the stability properties. Rigorous proofs of the linear stability calculations will be considered elsewhere [13].

Figure 2 illustrates numerical solutions of Eq. (1) for initial conditions consisting of the exact $\text{sn}(x, k)$ and

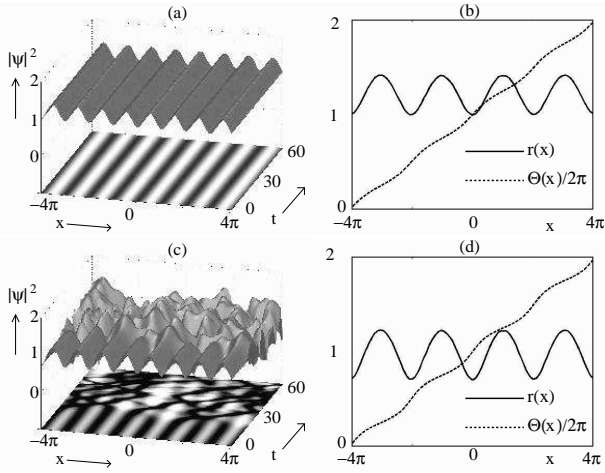


FIG. 3. Evolution of perturbed trigonometric solutions ($k = 0$) with nontrivial phase. In panels (a)–(b), $B = 1$ so that the solution is $\text{dn}(x, k)$ -like, leading to a stable evolution. The initial amplitude and phase are depicted in the top right. For $B = 1/2$, the solution is unstable, as seen in (c). Its initial phase and amplitude are depicted in panel (d). This indicates that a sufficiently high DC offset is required to stabilize the evolution.

$\text{dn}(x, k)$ solutions perturbed with a small amount of initial stochastic white noise, along with the corresponding Fourier spectra. Figures 2(c) and 2(d) depict the evolution of a $\text{sn}(x, k)$ initial condition perturbed by noise. For this simulation, $V_0 = 1$ and $k = 0$ so that the solution is a simple sinusoid (see Fig. 1). The solution is unstable, and diverges rapidly from the exact solution given in Eq. (6). From the plot of the Fourier spectrum, it is clear that the instability begins in a neighborhood of wavenumber $\eta = 1$ as predicted from the linear stability analysis. Similar behavior is observed for the $\text{cn}(x, k)$ branch of solutions. Figures 2(a) and 2(b) depict the evolution of the stable $\text{dn}(x, k)$ branch of solutions which is initially perturbed by white noise. In this simulation $V_0 = -1$ and $k = 1/2$. This solution branch is stable, and stays close to the exact solution for all time. Note that the Fourier spectrum is dominated by the zero mode, which determines the DC offset, and the wavenumber one, which determines the oscillation strength.

The Nontrivial Phase, Trigonometric Limit – For $k = 0$, $\text{sn}(x, 0) = \sin(x)$. The governing evolution Eq. (1) reduces to

$$i\psi_t = -\frac{1}{2}\psi_{xx} + |\psi|^2\psi - V_0 \sin^2(x)\psi. \quad (11)$$

Note that by the trigonometric identity $2\sin^2(x) = 1 - \cos(2x)$ this potential is sinusoidal. The solutions reduce to

$$\psi(x, t) = \sqrt{V_0 \sin^2 x + B} \exp[i(\Theta(x) - (1/2 + B)t)] \quad (12)$$

where

$$\tan(\Theta(x)) = \pm \sqrt{1 + V_0/B} \tan(x) \quad (13)$$

determines the nontrivial phase provided that $B \geq -V_0$ for $V_0 < 0$ and $B \geq 0$ for $V_0 > 0$.

The results of the previous section imply that the trivial phase solutions without offset are unstable. Oscillations about some mean value is qualitatively similar to a $\text{dn}(x, k)$ solution, which suggests that solutions with sufficiently large B might be stable. Oscillations with $|B|$ small are qualitatively like $\text{cn}(x, k)$ and $\text{sn}(x, k)$ and are expected to be unstable. Numerical experiments confirm this. We note that a linear stability analysis in this case is more complicated than for the trivial phase case since the linearized operators do not decouple as in Eq. (8).

In Fig. 3 we depict the evolution of a pair of initial conditions of the form given by Eq. (12) plus initial white noise. Figures 3(c) and 3(d) depict the initial amplitude and phase along with the evolution of the density $|\psi(x, t)|^2$ for the parameter values $V_0 = 1.0, B = 0.5$. It is clear from the graph that this stationary solution is unstable. Figures 3(a) and 3(b) depict the initial amplitude and phase and the evolution of the density for parameter values $V_0 = 1.0, B = 1.0$. In this case the solution appears stable. The solution with the perturbed initial condition stays close to the stationary solution for long times, which for our time scaling is longer than the lifetime of typical trapped BECs [2].

The numerical and analytical results imply that in order to obtain a stable condensate it is necessary to have solutions which are sufficiently in the nonlinear regime. To quantify this, we note that from Eqs. (11) and (12), the number of particles per well n is given by $n = (\int_0^\pi |\psi(x, t)|^2 dx) / \pi = V_0/2 + B$. In the context of the BEC, and for a fixed atomic coupling strength, this means a sufficient number of condensed atoms per well n is required to provide a DC offset on the order of the potential strength. This ensures stabilization of the condensate.

To demonstrate the physical viability of our results, we perform numerical simulations consistent with recent experiments on the BEC [6]. In particular, we consider a fixed number of condensed atoms with an initially constant DC profile. We adiabatically ramp up the periodic potential linearly from zero to a fixed potential strength V_0 . In an experiment, the condensate initially has a trivial phase profile and the solution deforms as depicted in Fig. 4(a). This adiabatic process generates a stable solution which is close to the $\text{dn}(x, k)$ solution branch given by Eq. (6b) and depicted in Fig. 2(a). In contrast, an initial DC profile with a nontrivial phase profile is only stable provided the DC

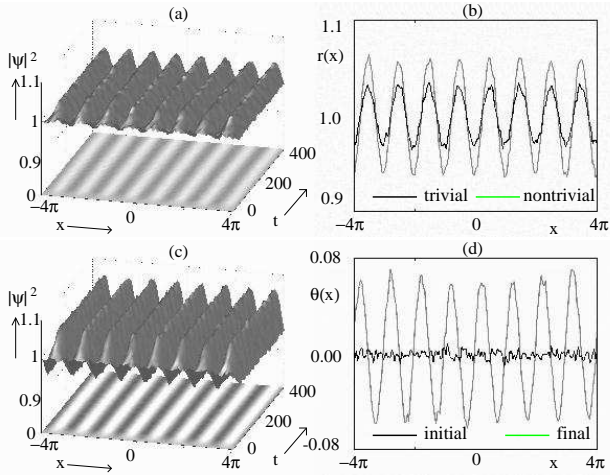


FIG. 4. Stable growth of periodic condensate with DC offset of one with (a) initial trivial phase and (c) nontrivial phase. A $\sin^2(x)$ potential was adiabatically grown from $V_0 = 0$ at $t = 0$ to $V_0 = 0.5$ at $t = 50$. Figure (b) shows the difference in the final state of the system given an initial trivial phase (black line) and initial nontrivial phase (gray line). The development of phase structure on an initial linear phase profile is depicted in (d). Here the initial linear phase profile has been subtracted out to give the initial (black line) and final (gray line) phase profiles.

offset is sufficiently large in comparison to the potential strength V_0 . For $V_0 = 0.5$ and an initial DC offset of one, the adiabatically grown solution is stable with larger amplitude fluctuations than those of the trivial phase case (Fig. 4b). As the condensate evolves, the initial linear phase profile is deformed as shown in Fig. 4(d), where the initial linear phase profile is subtracted out from the initial and final phases. This phase deformation is necessary in order for the solution to remain stationary. In particular, a linear phase profile induces a group-velocity shift in the direction of growing phase. This is in contrast to phase jumps or transition regions which can cause motion opposite the direction of a positive jump [2,5]. The stationary solutions generated here suggest that these two opposite actions effectively balance each other in order for the solutions to remain localized and stationary in their respective troughs. Finally, we note that for $V_0 = 1$ the potential is sufficiently strong so as to destabilize the adiabatically grown solution. The instability mechanism is similar to that observed in Fig. 3(c).

Conclusions – We have considered the repulsive NLS equation with a Jacobian elliptic function potential as a model for a trapped, quasi-one-dimensional Bose-Einstein condensate, and thereby produced a whole family of solutions. We have shown the stability of the $\text{dn}(x, k)$ branch of solutions rigorously. In addition, we have used a perturbative argument to show the instability of the $\text{sn}(x, k)$ and $\text{cn}(x, k)$ solutions. In the sinusoidal

limit we have provided numerical evidence that the nontrivial phase solutions are stable for sufficiently large offset B . Stable trivial and nontrivial phase trigonometric solutions can be obtained through adiabatic ramping of the potential strength provided there is a sufficient DC offset in the number of condensed atoms. As this models a Bose-Einstein condensate trapped in a standing light wave, our results imply that sufficiently large number of condensed atoms (DC offset) are required to form a stable, periodic condensate.

We benefited greatly from discussions with Ricardo Carretero-González, Keith Promislow, and William Reinhardt. The work of J. Bronski, L. D. Carr, B. Deconinck, and J. N. Kutz was supported by National Science Foundation Grants DMS-9972869, CHE97-32919, DMS-0071568, and DMS-9802920 respectively.

* to whom correspondence should be addressed

- [1] F. Dalfovo, S. Giorgini, L. P. Pitaevskii, and S. Stringari, *Rev. Mod. Phys.* **71**, 463 (1999).
- [2] L. D. Carr, M. A. Leung, and W. P. Reinhardt, *J. Phys. B* in press, e-print cond-mat/0004287 (2000).
- [3] M. Key *et al.*, *Phys. Rev. Letts.* **84**, 1371 (2000); N. H. Dekker *et al.*, *Phys. Rev. Letts.* **84**, 1124 (2000).
- [4] M. Kunze and *et. al.*, *Physica D* **128**, 273 (1999); Y. S. Kivshar, T. J. Alexander, and S. K. Turitsyn, e-print cond-mat/9907475 (1999).
- [5] L. D. Carr, C. W. Clark, and W. P. Reinhardt, *Phys. Rev. A* in press, e-print cond-mat/9911177, cond-mat/9911178 (1999).
- [6] B. P. Anderson and M. A. Kasevich, *Science* **282**, 1686 (1998); E. W. Hagley *et al.*, *Science* **283**, 1706 (1999).
- [7] Y. B. Ovchinnikov *et al.*, *Phys. Rev. Letts.* **83**, 284 (1999).
- [8] D. Jaksch *et al.*, *Phys. Rev. Letts.* **81**, 3108 (1998); G. K. Brennen, C. M. Caves, P. S. Jessen, and I. H. Deutsch, *Phys. Rev. Letts.* **82**, 1060 (1999).
- [9] D.-I. Choi and Q. Niu, *Phys. Rev. Letts.* **82**, 2022 (1999).
- [10] S. Theodorakis and E. Leontidis, *J. Phys. A* **30**, 4835 (1997); F. Barra, P. Gaspard, and S. Rica, *Phys. Rev. E* **61**, 5852 (2000).
- [11] K. Berg-Sørensen and K. Mølmer, *Phys. Rev. A* **58**, 1480 (1998); M. J. Steel and W. Zhang, e-print cond-mat/9810284 (1998).
- [12] *Handbook of Mathematical Functions*, edited by M. Abramowitz and I. A. Stegun (National Bureau of Standards, Washington, D. C. 1964).
- [13] J. C. Bronski, L. D. Carr, R. Carretero-González, B. Deconinck, J. N. Kutz and K. Promislow, *Phys. Rev. A*, to be submitted (2000).
- [14] M. Weinstein, *SIAM J. Math. Anal.* **16**, 472 (1985).